Chemistry Europe
European Chemical Societies Publishing

WILEY VCH

Excellence in Chemistry Research

Announcing our new flagship journal

- Gold Open Access
- Publishing charges waived
- Preprints welcome
- Edited by active scientists

Meet the Editors of *ChemistryEurope*

Luisa De Cola
Università degli Studi di Milano Statale, Italy

Ive Hermans
University of Wisconsin-Madison, USA

Ken Tanaka
Tokyo Institute of Technology, Japan

Chemistry–A European Journal
Research Article
doi.org/10.1002/chem.202202730
Chemistry Europe
European Chemical Societies Publishing
www.chemeurj.org

TEMPO-Modified Polymethacrylates as Mediators in Electrosynthesis: Influence of the Molecular Weight on Redox Properties and Electrocatalytic Activity

Adrian Prudlik,[a, b] Nayereh Mohebbati,[a, b] Laura Hildebrandt,[a] Alina Heck,[c, d] Lutz Nuhn,[c, d] and Robert Francke*[a, b]

Abstract: Homogeneous catalysts ("mediators") are frequently employed in organic electrosynthesis to control selectivity. Despite their advantages, they can have a negative influence on the overall energy and mass balance if used only once or recycled inefficiently. Polymediators are soluble redox-active polymers applicable as electrocatalysts, enabling recovery by dialysis or membrane filtration. Using anodic alcohol oxidation as an example, we have demonstrated that TEMPO-modified polymethacrylates (TPMA) can act as efficient and recyclable catalysts. In the present work, the influence of the molecular size on the redox properties and the catalytic activity was carefully elaborated using a series of TPMAs with well-defined molecular weight distributions. Cyclic voltammetry studies show that the polymer chain length has a pronounced impact on the key-properties. Together with preparative-scale electrolysis experiments, an optimum size range was identified for polymediator-guided sustainable reaction control.

Introduction

Indirect electrolysis using redox mediators is a frequently used approach toward controlling selectivity and reducing energy consumption of electro-organic transformations.[1] To address a multitude of synthetic problems, a well-established portfolio of mediators is available including organometallic compounds,[2] metal ions,[3] halides,[4] triarylamines,[5] iodoarenes,[6] and *N*-oxyl radicals.[7] Although the benefits of mediators are undisputed, they may be offset by more difficult separation procedures, increasing waste generation, and additional expenses, which is why concepts to facilitate separation and recycling deserve more attention.[8] The same applies to supporting electrolyte additives, which have to be removed by additional purification steps after completed reaction and, if not recycled, constitute a further source of waste.

The main challenge in recovering mediators from reaction mixtures is the similarity to the product in terms of polarity and molecular size. For example, column chromatography is required for separation of organic mediators such as iodoarenes or 2,2,6,6-tetramethylpiperidinyl-1-oxyl (TEMPO). In this regard, changing the polarity of the mediator by tethering charged groups ("ionic tags") has proven to be a promising approach that enables recovery by extraction while obviating the need for supporting electrolyte additives.[9] Further investigations focused on immobilization of mediators or supporting electrolytes on particles for electrolysis to be carried out in the dispersed phase.[10,11] While this approach allows for recovery by filtration or centrifugation, it is associated with drawbacks such as poor ionic conductivity and difficult electron transfer between electrode and immobilized mediator, respectively. Noteworthy, activation of mediators that are attached to suspended particles requires a homogeneous co-mediator,[10e,f] partially nullifying the benefits achieved by immobilization.

In view of the difficulties caused by the dispersed-phase approach, the installment of mediators on soluble polymer backbones is an interesting alternative, since the resulting polymediators can act as classic homogeneous electrocatalysts that are activated at the electrode surface and react with the substrates in solution. Simultaneously, the increased molecular size allows the use of size exclusion membrane processes for mediator recovery (i.e., dialysis and ultra-/nanofiltration).

Based on the TEMPO-catalyzed anodic alcohol oxidation, we have shown for the first time that indirect electro-organic reactions can efficiently be coupled to dialysis and ultrafiltration

[a] *A. Prudlik, N. Mohebbati, L. Hildebrandt, Prof. Dr. R. Francke*
Leibniz Institute for Catalysis
Albert-Einstein-Str. 29a, 18059 Rostock (Germany)
E-mail: Robert.francke@catalysis.de
[b] *A. Prudlik, N. Mohebbati, Prof. Dr. R. Francke*
Institute of Chemistry
Rostock University
Albert-Einstein-Str. 3a, 18059 Rostock (Germany)
[c] *A. Heck, Prof. Dr. L. Nuhn*
Max Planck Institute for Polymer Research
Ackermannweg 10, 55128 Mainz (Germany)
[d] *A. Heck, Prof. Dr. L. Nuhn*
Chair of Macromolecular Chemistry
Faculty of Chemistry and Pharmacy
Julius-Maximilians-Universität Würzburg
Röntgenring 11, 97070 Würzburg (Germany)

Supporting information for this article is available on the WWW under https://doi.org/10.1002/chem.202202730

when polymediators are employed (Figure 1A–C).[12] Trialkylammonium- and TEMPO-modified polymethacrylates (PTE and TPMA, Figure 1B), which can both be easily prepared on a decagram scale by free radical polymerization, served as polymediators and polyelectrolytes, respectively. The resulting polymer solutions turned out to be sufficiently conductive and exhibited a high electrocatalytic activity toward conversion of various alcohols to the corresponding carbonyl compounds. Recycling tests showed that the polymer solution can be reused multiple times.

In a subsequent electroanalytical study,[13] progress was made in understanding the redox behavior and catalytic activity of TEMPO-modified polymethacrylates using a sample with a number average molecular weight (M_n) of 3.6 kDa and a dispersity ($Đ$) of 1.29 (3.6-TPMA). First, it was found that the polymer adsorbs on the carbon electrode surface, which strongly influences the voltammetric profiles at low mediator concentration and at high scan rates. However, the linear relationship between catalytic current and concentration of TEMPO units suggested that under electrolysis conditions, TPMA-catalyzed alcohol conversion is predominantly a homogeneous process despite polymer adsorption. Second, TPMA shows a significantly slower diffusion rate compared to low molecular *N*-oxyls such as TEMPO and 4-acetoxy-TEMPO (ACT). Third, on average, the achievable catalytic current densities j_{max} are intermediate between those of TEMPO and ACT despite the smaller diffusion coefficient. The homogeneous rate constants k_{cat} of TPMA and ACT that were extracted from j_{max} for five tested substrates are similar to each other and exceed the ones of TEMPO. This suggests *i*) that the redox potential of the mediator unit has a stronger impact on the homogeneous rates than steric effects of the polymer backbone and *ii*), that curbed mass transfer can in part be compensated by tuning the redox potential of the catalyst unit.

As mentioned above, the results provided by the previous electroanalytical study were obtained from a single TPMA sample with a defined M_n distribution, whereby the relationship between the molecular weight and the electrocatalytic properties thus far remained unknown. Exploring this issue is of great importance, since the molecular weight seems to exert a significant impact on the catalysts diffusion, which is why an impact on the catalytic rate can be expected. Thus, from an electrocatalytic point of view, polymediators with rather small molecular weights appear to be advantageous, whereas larger polymers are desirable with respect to their recovery using size exclusion membranes. In view of these two opposing trends, optimization of the molecular weight appears to be of great importance to find a reasonable compromise between catalytic rates and recyclability. However, no study is yet available on the relationship between the molecular weights of polymediators and their electrocatalytic properties. In general, little is known to date about the influence of molecular size on the behavior of redox-active polymers, even though there is currently a high interest in these materials from further ends, for example in the fields of bioelectrochemistry[14] and electrochemical energy storage.[15] In a seminal work by Bard et al., the influence of the molecular weight on the electrochemical properties of dissolved poly(vinylferrocene) samples was investigated.[16] Later, Rodríguez et al. characterized soluble viologen-modified polystyrenes with varying chain lengths with respect to their redox activity and transport through porous membranes for potential application in redox flow batteries.[17] TPMAs with varying molecular weights have also been systematically characterized, however, thus far exclusively in the solid state as part of composite electrodes with regard to applications in organic radical batteries.[18] Given the limited available knowledge, we have carried out a detailed analysis of the relationship between the key-properties of TPMA-based polymediators and their molecular size, the results of which are presented herein.

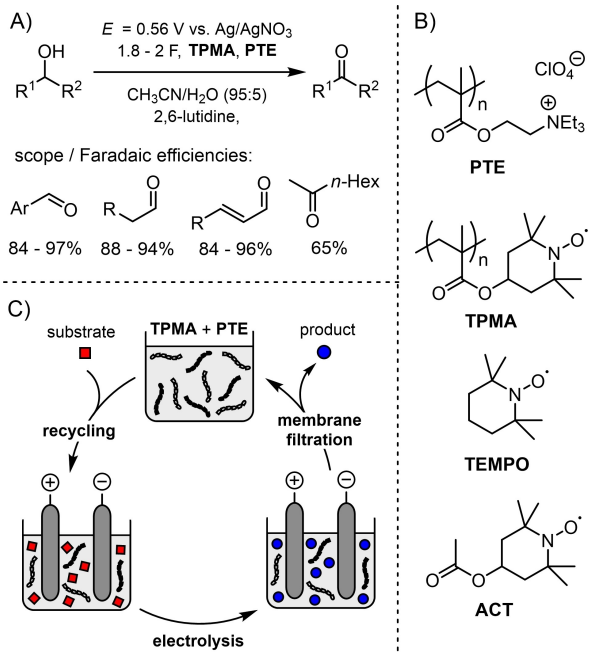

Figure 1. Concept of indirect electrolysis using polymediators and polyelectrolytes.[12,13] A) Preparative-scale anodic oxidation of alcohols using polymediators (TPMA) and polyelectrolytes (PTE).[12] B) Polyelectrolyte and *N*-oxyls under investigation in previous works. C) Schematic illustration of the electrolysis and recycling procedure.

Results and Discussion

In our initial feasibility study,[12] TPMA was synthesized via a free radical polymerization of commercially available 2,2,6,6-tetramethylpiperidin-4-yl-methacrylate (**1**), followed by oxidative conversion of the piperidinyl units into *N*-oxyl radicals. The polymerization step involved 2-mercaptoethanol as a modifier, resulting in an M_n value of 1.45 kDa after the oxidation step.[19] In terms of reaction conditions, this approach is very robust, easy to perform, and well scalable. However, it provides only limited control over the length of the polymer chain, which is reflected by a broad molar mass distribution ($Đ = 1.89$). For our subsequent investigation,[13] the dispersity was reduced by RAFT polymerization[20] to exclude possible influences of large molecular weight differences ($M_n = 3.6$ kDa, $Đ = 1.29$). The same

approach has been used in this work to adjust the molecular weights properly (see Scheme 1).

Polymerization of hydrochloride **1·HCl** was achieved using AIBN as a radical starter and dithioester **2** as a chain transfer reagent, followed by oxidation of the resulting intermediate PTM·HCl to yield the desired TPMAs. Since during oxidation with H_2O_2/$NaWO_4$ under alkaline conditions, the intermediate precipitated prior to complete oxidation, the solid was filtered off and dissolved in THF, where the conversion was brought to completion by addition of mCPBA. UV-vis spectroscopic studies confirmed that PTM·HCl initially contains intact thiobenzoylthio end groups, which are cleaved off during reaction to TPMA.[13] End group removal under alkaline and oxidative conditions is also in agreement with literature reports on the stability of thiobenzoylthio moieties.[21] Further details on preparation, purification, and characterization of the polymers are provided in the Supporting Information.

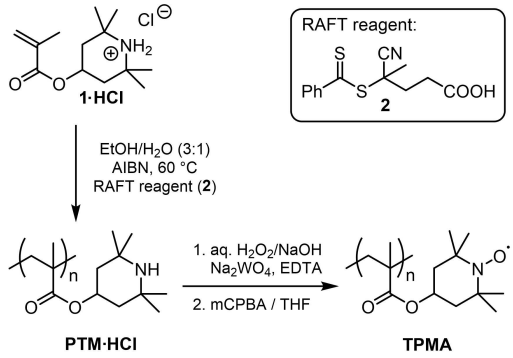

Scheme 1. Preparation of TPMA from monomer **1·HCl**.

Table 1. Results of the two-step polymer syntheses shown in Scheme 1.

Polymer sample	**2** [mol-%]	M_n [kDa]	$Đ$
2.5-TPMA	3.89	2.5	1.16
3.6-TPMA	1.57	3.6	1.30
11.5-TPMA	1.40	11.5	1.38
14.9-TPMA	1.24	14.9	1.45
15.0-TPMA	0.93	15.0	1.32
16.0-TPMA	1.09	16.0	1.44
19.6-TPMA	0.62	19.6	1.31
26.6-TPMA	0.83	26.6	1.25
30.0-TPMA	0.32	30.0	1.30
30.8-TPMA	0.46	30.8	1.29
62.0-TPMA	0.18	62.0	1.26
71.3-TPMA	0.24	71.3	1.26
94.3-TPMA	0.12	94.3	1.34
111.3-TPMA	0.03	111.3	1.99
126.0-TPMA	0.06	126.0	1.68

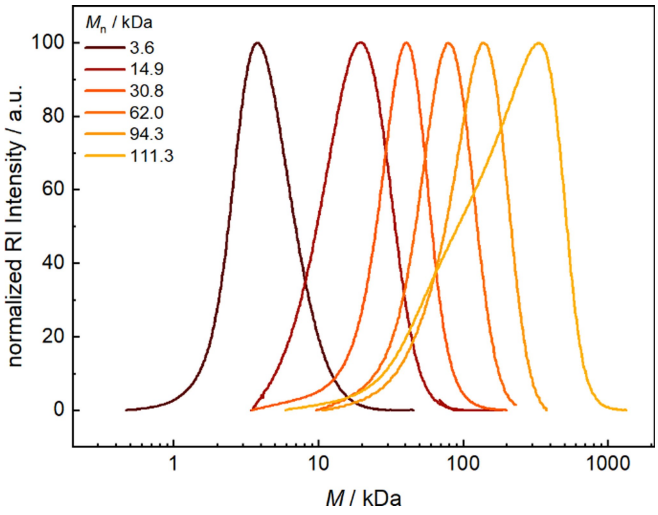

Figure 2. Molecular weight distributions of representative TPMAs (for a complete overview, see the Supporting Information).

The molar mass of the polymers was adjusted by varying the ratio between monomer and chain transfer agent, obtaining a total of 15 samples with M_n values ranging from 2.5 to 126.0 kDa (see Table 1) in isolated yields between 48% and 94% calculated with respect to **1·HCl**. All TPMA samples exhibited a monomodal molecular weight distribution as illustrated by the examples of Figure 2. While the $Đ$ values range from 1.16 to 1.45 for the TPMAs with $M_n < 111.3$ kDa, the two samples with highest M_n provided increased dispersities. The latter is expectable, since low concentrations of RAFT reagents frequently result in a decreased control over radical polymerization.

The electrochemical properties of the TPMA samples were studied by cyclic voltammetry (CV) using a glassy carbon working electrode and a Ag/0.01 M $AgNO_3$ reference electrode ($E_0 = -87$ mV vs. Fc/Fc^+ couple).[22] A 0.1 M solution of NBu_4ClO_4 in a mixture of CH_3CN and water (8:1 vol/vol) served as the electrolyte, in which the polymer content was adjusted to an effective concentration of polymer units (c_{TU}) of 5 mM. To allow a comparison between the TPMAs and low-molecular-weight TEMPO species, 4-acetoxy TEMPO (ACT) and a TEMPO dimer (BTM, see Figure 3A) were subjected to the same analysis. The CVs of ACT, BTM, and four representative polymers (3.6-, 15.0-, 30.8-, and 126.0-TMPA) recorded at 100 mV s^{-1} are shown in Figure 3(B) (key-parameters are summarized in Table 2). Each species exhibits a single reversible redox couple (R_2N–$O^•$/R_2N=O^+), which suggests that there is no significant electronic interaction between the TEMPO units along the polymer backbone.[23] The voltammetric profiles show diffusive character, high chemical reversibility (peak current ratio $j_{p,c}/j_{p,a}$ close to unity, see Table S2), and similar equilibrium redox potentials (E_0, situated in the range between 0.40 V and 0.43 V), suggesting that at 100 mV s^{-1}, the behavior of ACT, BTM, and the PTMAs is essentially the same. That redox-active polymers can exhibit the

Table 2. Parameters extracted from the CVs of the TEMPO species. The shown values are mean values of two measurements.

Species	E_0 vs. $Ag/AgNO_3$[a] [V]	$j_{p,a}$[a] [mA cm^{-2}]	D [cm^2 s^{-1}]
ACT	0.40[b]	1.76[b]	1.53×10^{-5}[b]
BTM	0.41	1.22	7.76×10^{-6}
3.6-TPMA	0.43	0.65	2.36×10^{-6}
15.0-TPMA	0.41	0.45	1.10×10^{-6}
30.8-TPMA	0.42	0.36	7.24×10^{-7}
126.0-TPMA	0.42	0.16	1.37×10^{-7}

[a] Estimated at 100 mV s^{-1}. [b] Values taken from Ref. [13].

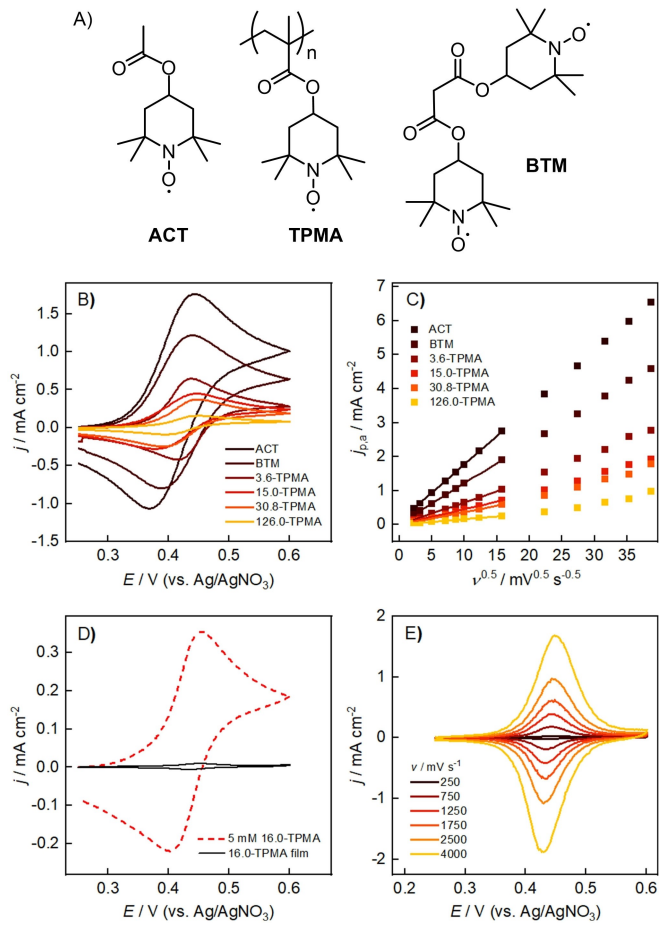

Figure 3. Cyclic voltammetry (CV) of selected *N*-oxyls in a solution of 0.1 M NBu_4ClO_4 in CH_3CN/H_2O (8:1, vol/vol). A) Structures of analyzed species. B) CVs of ACT, BTM, 3.6-, 15.0-, 30.8-, and 126.0-TPMA recorded at 100 mV s^{-1} (c_{TU} = 5 mM). C) Plot of the anodic peak current densities ($j_{p,a}$) vs. $v^{0.5}$. D) CV of 5 mM 16.0-TPMA (red line) recorded at 100 mV s^{-1} and repeated scan after replacing the solution with blank electrolyte (black line). E) CVs of adsorbed 16.0-TPMA recorded at various scan rates.

same form of current-potential responses as molecules with only one corresponding center has already been observed in other studies, for example, in the electrochemical analysis of poly(vinylferrocene).[16]

Large differences are noticeable when comparing the current densities (j) of the CVs, which, starting from ACT, decrease with increasing molar weight. This trend suggests that the availability of redox-active units at the electrode surface decreases for the higher-molecular-weight TEMPOs, which may result from curbed mass transfer. This behavior also becomes evident upon varying the scan rate (Figure 3C). Furthermore, with a stepwise increase of v, an additional peculiarity is noticeable: While up to 250 mV s^{-1}, ACT, BTM, and the TPMAs show a linear relationship between the anodic peak current density ($j_{p,a}$) and $v^{0.5}$, a deviation from the square root dependency occurs exclusively for the TPMAs above 250 mV s^{-1}. This deviation results from a superposition of adsorptive and diffusive processes, i.e., from charge transfer to both dissolved and adsorbed polymer chains, and has been studied in detail in our previous work.[13] Consequently, the square root dependency of $j_{p,a}$ at low scan rates indicates that at large time scales, the major part of the charge is transferred in diffusive processes. On the other hand, the adsorptive fraction of $j_{p,a}$ that increases linearly with v[24] becomes more pronounced at higher scan rates.

To confirm that adsorption of TPMAs on the electrode surface is responsible for the deviation from the square root dependency, additional experiments were performed in which CVs were first recorded in a TPMA solution (c_{TU} = 5 mM), followed by careful rinsing of the electrode with acetonitrile, immersion into a blank electrolyte solution, and repeated cycling. The results are shown exemplarily for 16.0-TPMA: While at 100 mV s^{-1}, voltammetry in the blank electrolyte shows only an extremely weak signal (Figure 3D, black line), well-defined and nearly symmetric features centered around 0.43 V become apparent at high scan rates (Figure 3E). These features exhibit only a small splitting between the oxidative and the reductive peak ($\Delta E_p \sim 15$ mV), which is typical for independent and identical redox-active species attached to the electrode surface.[25] The apparent surface concentration of TEMPO units (Γ_{TU}) calculated from the charge obtained via integration of the anodic peak of the CV recorded at 750 mV s^{-1} corresponds to 1.42×10^{-10} mol cm^{-2}. This value is in the same order of magnitude but well below sterically limited Γ values reported for monolayers of other redox-active molecules (e.g., ferrocene) covalently attached to smooth surfaces.[26] The profiles do not change significantly over ten cycles, indicating high stability of the TPMA layer on the experimental time scale (see Figure S3). The same effect has already been observed in our previous study on 3.6-TPMA.[13] Consequently, polymer adsorption seems to be a general effect that occurs independently from the M_n value of the polymer.

For a quantitative comparison between the transport properties, the diffusion coefficients D of the different TEMPO species were calculated from the slope of the j_p vs. $v^{0.5}$ plot using Equation (1),[25]

$$j_p = 0.4463 z F c_{TU} \sqrt{\frac{zFvD}{RT}} \quad (1)$$

where z corresponds to the number of transferred electrons per TEMPO unit (z = 1), F to the Faraday constant, R to the ideal gas constant, and T to the temperature (the other parameters are defined above). It should be noted that c_{TU} is kept constant (5 mM) and that for the polymer samples, the treatment renders apparent diffusion coefficients that refer to individual TEMPO units rather than to entire polymer chains.[12,13,17] To exclude influences of adsorption, only the v range dominated by the diffusive process is evaluated (5–250 mV s^{-1}, see Figure 3C). The resulting D values are summarized in Table 2 for the selected examples and in Figure 4 for all studied *N*-oxyl species.

In principle, smaller diffusion coefficients are observed with increasing molecular weight of the polymer, with a rapid initial drop that leads to a 95% decrease in D for 19.6-TPMA compared to ACT (Figure 4A). The profile shown is well explained when considering the relationship between D and

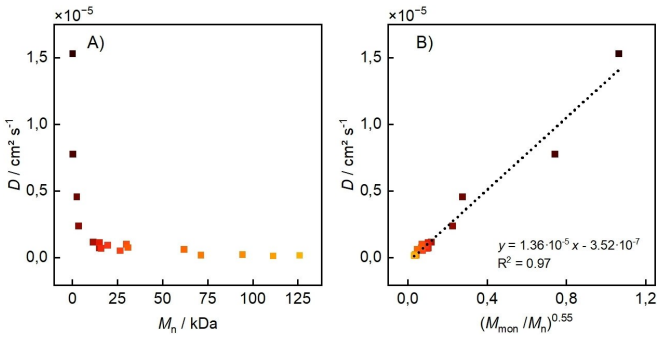

Figure 4. Plot of the diffusion coefficients *D* derived from Randles-Sevcik analysis vs. A) M_n and B) M_{mon}/M_n. The shown *D* values are mean values from twofold estimations.

the hydrodynamic radius *r* of a diffusing species according to the Stokes-Einstein equation ($D \sim r^{-1}$), and substituting *r* by M_n^a using scaling theory with *a* being the Flory exponent ($a = 0.5$ for ideal random polymer coils in a theta solvent and $a = 0.6$ for swollen coils in a good solvent).[27] In practice, the following empirical relationship has proven useful,

$$\frac{D}{D_{mon}} = \left(\frac{M_{mon}}{M_n}\right)^{0.55} \quad (2)$$

which relates *D* to M_n, the (hypothetical) diffusion coefficient, and the molecular weight of the monomer unit (D_{mon} and M_{mon}, respectively).[16–17] In the context of the abovementioned Stokes-Einstein equation and scaling relation, the exponent 0.55 would represent a scenario in which the polymer chain is randomly coiled in a good solvent ($0.5 < a < 0.6$).

As can be seen from the plot in Figure 4(B), *D* varies linearly with respect to the 0.55 power of the ratio between M_n and M_{mon}. The slope of the linear fit corresponds to D_{mon} and with 1.49×10^{-5} cm^2 s^{-1}, it is well comparable to the diffusion coefficient of the model monomer ACT ($D_{ACT} = 1.72 \times 10^{-5}$ cm^2 s^{-1}). Together with a negligible y-axis intercept (-3.52×10^{-7} cm^2 s^{-1}) and an R^2 value of 0.97, the linear fit is in good agreement with the behavior predicted by Equation (2). Since Equation (2) originally refers to regular diffusion coefficients of polymers, and the *D* values summarized in Figure 4 are to be considered as apparent diffusion coefficients of individual TEMPO units, some caution must be exercised in interpreting Figure 4(B). However, it seems reasonable to conclude that the observed relationship reflects the impact of the molecular weight on the rate of mass transfer and thereby on the diffusion-limited peak current density. In other words, the relationship between M_n and *D* follows the behavior predicted by the Stokes–Einstein equation in the sense that diffusion is curbed with increasing molecular size. In view of applications in homogeneous electrocatalysis, the profile shown in Figure 4(A) illustrates that polymers with M_n values smaller than approx. 10 kDa exhibit promising diffusion behavior, whereas diffusion coefficients of larger TPMAs appear rather unfavorable.

The study was continued by analyzing the impact of the molecular weight on the electrocatalytic behavior of the TPMAs. For this purpose, 4-methoxybenzyl alcohol (4-MBA) was used as a test substrate. A comparison between the voltammetric profiles of four representative examples, ACT, BTM, 3.6-, and 26.6-TPMA, recorded at 100 mV s^{-1} in the absence and presence of the alcohol substrate is shown in Figure 5. *N*-Methylimidazole (NMI) was added as a proton scavenger to enable electrocatalytic alcohol oxidation. A control CV recorded without mediator confirmed that direct (uncatalyzed) anodic substrate conversion does not occur in the studied potential range (see Figure S5). In all cases, a typical catalytic response is seen (solid line), where indirect oxidation of the alcohol enhances the anodic current compared to the non-catalytic CV (dashed line), and where the cathodic peak disappears in the reverse scan. Upon comparing the profiles, it becomes clear that *i*) significant catalytic currents can be achieved both with ACT as well as with

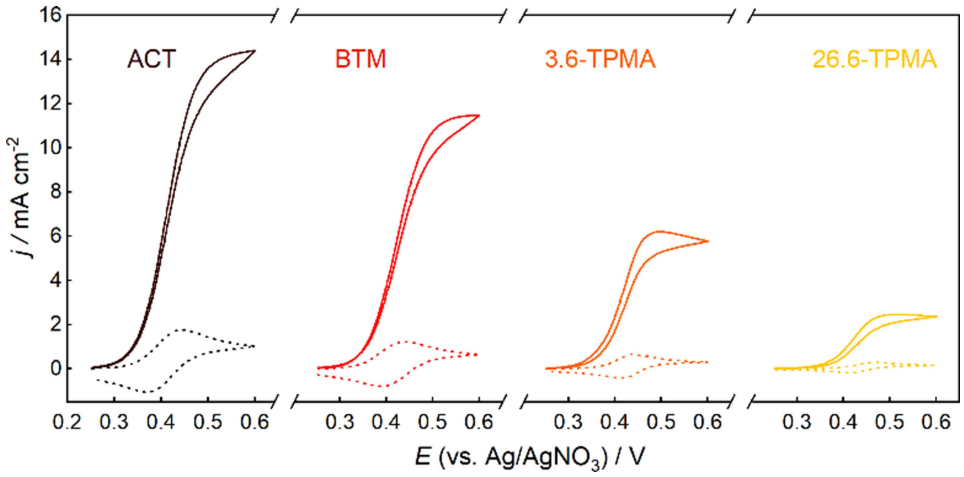

Figure 5. CVs of ACT, BTM, 3.6-TPMA, and 26.6-TPMA, recorded at 100 mV s^{-1}. Conditions: $c_{TU} = 5$ mM, 0.1 M NBu_4ClO_4 in CH_3CN/H_2O (8:1, vol/vol) in the absence (dashed) as well as in the presence of 0.1 M 4-MBA and 0.45 M NMI (solid line).

higher molecular weight TEMPO species and *ii*), that the catalytic peak current densities j_{cat} decrease with increasing molecular size. The latter occurs concomitantly with decreasing $j_{p,a}$ values, whereby the current enhancements do not differ greatly ($j_{cat}/j_{p,a}$ between 8.2 and 9.6). This suggests that the overall reaction rate decreases with increasing M_n due to a curbed diffusion of the mediator.

The catalytic behavior was studied in more detail by variation of the scan rate. In Figure 6(A), the progression of the catalytic response is shown exemplarily for 15.0-TPMA. While initially, an increase in v leads to a strong current enhancement, the profiles remain nearly unchanged at higher scan rates. Together with the canonical S-shape of the curves, this suggests that at high scan rates und sufficiently high electrode potential, only the kinetics of alcohol oxidation determine the current response ('pure kinetic conditions').[28] The same progression of the catalytic profiles is observed for ACT and BTM as well as for the other TPMAs (see the Supporting Information).

Figure 6(B) shows the plots of j_{cat} vs. v for seven representative TEMPO species. Comparison between the plots highlights the relationship between molecular weight and electrocatalytic activity. In all cases studied, j_{cat} reaches a plateau value (j_{max}) at high scan rates. The plot of j_{max} against M_n (Figure 6C) initially shows a sharp drop from 16.3 mA cm^{-2} (ACT) to 6.1 mA cm^{-2} (15.0-TPMA), whereas the decrease is significantly attenuated toward higher M_n values. Interestingly, even polymers with M_n > 60 kDa achieve appreciable j_{max} values despite their extremely low diffusion coefficients. For example, 126.0-TPMA as the largest polymer with a D value of only 1.41×10^{-7} cm^{-2} (as compared to 1.53×10^{-5} cm^{-2} for ACT) still achieves a j_{max} value of 3.2 mA cm^{-2}.

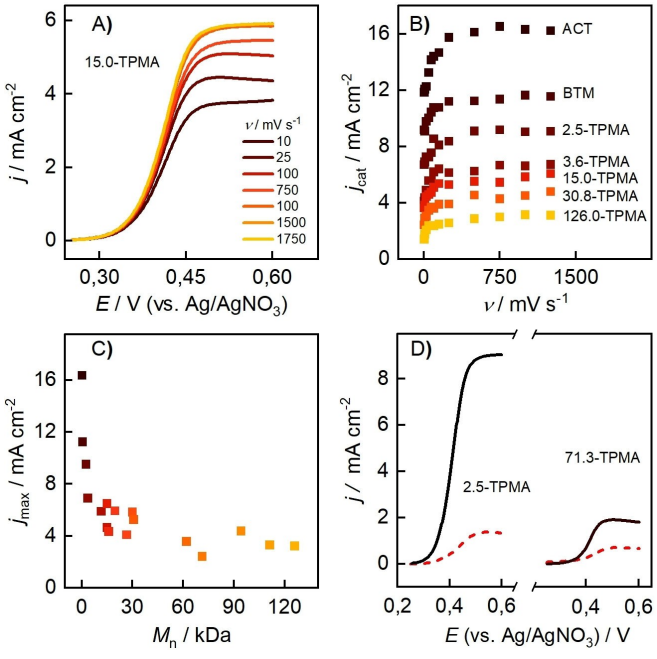

Figure 6. A) LSVs of 15.0-TPMA, recorded at various scan rates. Conditions: c_{TU} = 5 mM, 0.1 M NBu_4ClO_4 in CH_3CN/H_2O (8:1 vol/vol), 0.1 M 4-MBA, and 0.45 M NMI. B) Maximum achievable current densities (j_{cat}) vs. the scan rate for ACT, BTM, and five representative polymers. C) Plot of the plateau current densities achieved under pure kinetic conditions (j_{max}) against M_n (the shown j_{max} values are mean values from two measurements). D) LSVs of 5 mM 2.5-TPMA and 71.3-TPMA recorded at 1 V s^{-1} in presence of 4-MBA and base (black solid line); repeated scan after replacing the solution with TPMA-free, substrate- and base-containing solution (red dashed line).

Assuming pure homogeneous electrocatalysis, j_{max} is given by the following equation,[28a,29]

$$j_{max} = zFc_{TU}\sqrt{nDk_{cat}c_{sub}} \quad (3)$$

with k_{cat} as the homogeneous rate constant, n as the number of catalyst units required per turnover, and c_{sub} as the substrate concentration (the other parameters are defined above). Regarding Equation (3), it appears tempting to determine k_{cat} values for the polymediators. However, in view of the polymer adsorption described above (Figure 3D), caution should be exercised in the kinetic analysis of TPMA-catalyzed reactions. The influence of adsorbed TPMA on the catalytic response is illustrated in Figure 6(D) using the catalytic responses of 2.5-TPMA and 71.3-TPMA recorded at 1 V s^{-1} as examples. In both cases, the measurement was carried out under the same conditions as in Figure 6(A) (black solid lines), followed by removal and rinsing of the electrode, and repeated scan after replacing the electrolyte with a TPMA-free but substrate- and base-containing solution (red dashed lines). A comparison of the profiles recorded before and after change of the solution shows that TPMAs attached to the electrode participate in substrate oxidation, whereby the heterogeneous contribution to j_{cat} is much more pronounced for 71.3-TPMA (35%) than for 2.5-TPMA (15%).

Similar to homogeneous electrocatalysts, adsorbed molecular catalysts exhibit S-shaped profiles under pure kinetic conditions.[28c] An anodic process catalyzed only by adsorbed TEMPO species would lead to plateau currents given by Equation (4),[28b]

$$j_{max} = nF\Gamma_{TU}k_{cat}c_{sub} \quad (4)$$

where Γ_{TU} corresponds to the surface concentration [mol cm^{-2}] of TEMPO units and the other parameters have been defined above. Assuming that no interactions exist between the homogeneously and heterogeneously electrocatalytic processes, the procedure shown on Figure 6(A and D) would in principle allow separation of the contributions of dissolved and adsorbed TPMAs (and thus determination of the homogeneous and heterogeneous k_{cat} values). However, since the catalytic currents of adsorbed TPMAs in TPMA-free solutions are not stable over several cycles, analysis of the individual contributions is not feasible. Still, the j_{max} values summarized in Figure 6(C) are well-suited for characterization of the macroscopic kinetics since they reflect the overall reaction rate as an interplay between catalyst diffusion and microscopic rate.

The previously discussed CV results have proven useful in elucidating the influence of molecule size on redox behavior, transport processes, and electrocatalytic properties. The knowledge gained and intrinsic parameters determined are important for the mechanistic understanding and for the comparison of

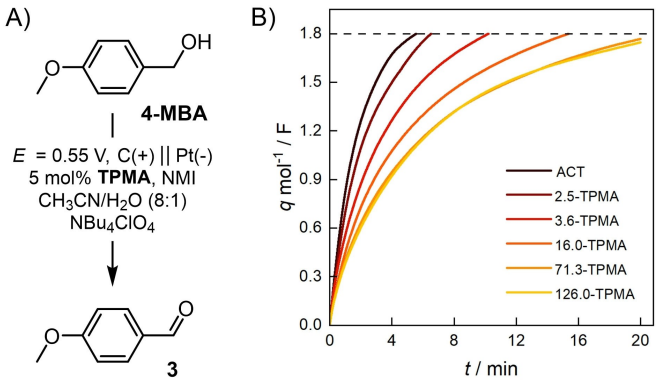

Figure 7. A) TPMA-catalyzed anodic oxidation of 4-MBA to anisaldehyde (**3**) under potentiostatic conditions. B) Corresponding charge-time profiles for ACT and different TPMAs. Electrolyte: 0.1 M Bu_4NClO_4 in CH_3CN/H_2O (8:1, v/v), anode: carbon roving, divided cell, rt. $E = 0.55$ V vs. $Ag/AgNO_3$, 0.075 M 4-MBA (batch size: 0.75 mmol), 0.11 M NMI.

the different *N*-oxyl species. However, it should also be considered that the conditions in preparative-scale applications are significantly more complex than in the CV experiments. Particularly noteworthy are the change of the electrolyte composition during electrolysis as well as forced convection for improved mass transfer. To gain a better insight into the behavior under preparative conditions, controlled potential electrolyses (CPE) were carried out at $E = 0.55$ V with different TPMAs in the presence of 4-MBA (Figure 7A). A divided cell was used in combination with a carbon roving anode[30] and a platinum cathode. An inexpensive size exclusion membrane made of regenerated cellulose served as a separator (for more information see the Supporting Information). The corresponding charge-time profiles are depicted in Figure 7(B). The time periods required to pass 1.8 F per mole of substrate are summarized in Table 3 along with the corresponding Faradaic efficiencies (*FE*).

In all cases, *FE*s between 78% and 95% were achieved. A comparison of the charge-time profiles demonstrates the effect of the molecular weight on the reaction rate. While the electrolysis time differed little between ACT (5.6 h) and 2.5-TPMA (6.6 h), it increased dramatically upon using longer polymer chains. When 71.3- and 126.0-TPMA were employed, electrolysis was stopped after 20 h, achieving a charge transfer of merely 1.77 F and 1.75 F, respectively. Taken together, the CPE experiments show that smaller TPMAs render attractive reaction times and *FE* values. Particularly with 2.5-TPMA, only minimal changes in overall reaction rate can be observed compared to ACT, a very encouraging result in view of future synthetic applications. In contrast, the results obtained with the larger TPMA's are less promising. Especially for 71.3-TPMA and 126.0-TPMA, reactions with $t > 20$ h are inacceptable. The experiments thus highlight the outstanding significance of the M_n distribution for the development of polymediator-guided electrochemical syntheses.

Table 3. Summary of the results of the electrolysis experiments shown in Figure 7.

Species	*q* per mole **4-MBA** [F]	Electrolysis time [h]	*FE* [%][a]
ACT	1.8	5.6	78
2.5-TPMA	1.8	6.6	79
3.6-TPMA	1.8	10.2	93
16.0-TPMA	1.8	15.4	95
71.3-TPMA	1.77	20.0	93
126.0-TPMA	1.75	20.0	80

[a] Faradaic efficiency determined via GC-FID analysis using an internal standard.

Conclusion

In the present study, progress has been made in understanding electrocatalysis involving TEMPO-modified polymethacrylates (TPMA) as mediators. It was shown how the molecular weight affects the key properties of the polymers, revealing that this aspect plays an important role in the development of poly-mediated processes. At this point, it is worth summarizing the most important findings:

1. Cyclic voltammetry is shown to be a simple and effective method for studying the key-properties of polymediators. At low to medium scan rates, the non-catalytic voltammetric profiles of the studied TPMAs are very similar to 4-acetoxy-TEMPO (ACT) in terms of equilibrium potential, chemical reversibility, and diffusive character, indicating a non-interacting electron exchange between electrode and TEMPO units attached to the polymer chain. Major differences between the TPMAs are observed for the achievable redox currents, which is explained by a decrease of the diffusion rate with increasing molecular size, following the behavior predicted by the Stokes–Einstein equation. In other words, short-chain TPMAs can be more rapidly charged than the larger polymers.
2. To quantify the effect of number-average molecular weight (M_n) on the diffusion rate, diffusion coefficients (*D*) conveniently estimated via CV turned out useful. For the TPMA series, the relationship between *D* and M_n is in good agreement with an empirical equation reported in the literature representing random coil polymers in good solvents.[16,27]
3. The affinity of the polymer to the electrode surface should be taken into account when studying reactions involving polymediators. In the present case, all TPMAs tend to adsorb on the electrode surface regardless of molecular weight. Polymer adsorption affects the non-catalytic voltammetric response, especially at low TPMA concentrations and high scan rates. Both dissolved and adsorbed TPMAs participate in the catalytic process, whereby the relative heterogeneous contribution is small for short-chain TPMAs and increases with increasing M_n.
4. The catalytic currents diminish with increasing molecular weight, which can be assigned to the decreasing diffusion coefficients. The maximum achievable catalytic current under pure kinetic conditions (j_{max}) is a parameter that can be conveniently determined for all *N*-oxyl species and reflects the interplay between catalyst diffusion, homoge-

neous rate, and catalysis by adsorbed TEMPO units. It can therefore serve as a useful measure for comparing the activity of the polymediators. Compared to ACT, the long-chain TPMAs provide only about one-fifth of the j_{max} value. In contrast, good results are achieved with shorter chains (2.5 and 3.6 kDa).

5. The trends observed in the CV studies translate well to controlled potential electrolysis. While all polymers provide good to very good Faradaic efficiencies, the electrolysis time prolongs with increasing molecular weight. Promising results were obtained with short-chain polymers (2.5 and 3.6 kDa), whereas the large TPMAs tend to give low currents and long reaction times.

Together with our previous mechanistic work on the subject,[13] it is now possible to assemble a coherent picture. From the insights gained, important criteria and design principles can be derived for future developments.

The current work clearly shows that short-chain polymediators are needed to achieve useful reaction rates, with consequences for coupling between electrolysis and membrane filtration (the latter serving to separate and recycle the polymers). Preliminary recycling studies on short-chain TPMAs using dialysis with commercially available porous size-exclusion membranes (regenerated cellulose, molecular weight cut-off: 1 kDa) already yielded promising results.[12] However, in pressure-driven ultrafiltration using the same membrane material, short-chain TPMAs were not sufficiently retained to enable multiple reuse with stable electrolysis performance. Thus, nanofiltration with dense membranes seems more suitable for quantitative recovery. However, more studies on polymer recovery and recycling are needed before applying the concept under industrially relevant conditions. For the latter, a continuous process in which an electrochemical flow reactor is coupled with a cross-flow membrane filtration cell appears particularly promising. Efforts to advance polymediator-guided electrosynthesis are ongoing in our laboratory.

Experimental Section

General remarks: All chemicals were purchased from Alfa Aesar, Sigma Aldrich or TCI and used as received. The supporting electrolyte (tetrabutylammonium perchlorate) was purchased from Sigma Aldrich in electrochemical grade. Acetonitrile was purchased in HPLC grade from Acros Organics and used as received. Synthesis and spectroscopic characterization of the TEMPO catalysts is described in the Supporting Information.

Size exclusion chromatography (SEC): The polymer samples were dissolved in 1,1,1,3,3,3-hexaflouropropan-2-ol (HFIP) (Fluorochem, Hadfield, UK) containing 3 gL^{-1} of potassium trifluoroacetate. The SEC instrument was equipped with a PU2080+ pump, an auto sampler AS1555 and an RI-detector RI2080+ from JASCO. Columns packed with modified silica were obtained from PSS (Mainz, Germany): PFG columns, particle size 7 μm, porosity 100 Å and 1000 Å. The column was kept in an oven at constant temperature of 40 °C. Calibration was carried out with poly(methyl methacrylate) (PMMA) standards, purchased from PSS (Mainz, Germany). The samples were prepared at 1–2 mg mL^{-1} and filtered through PVDF syringe filters (pore size 0.2 μm) prior to analysis.

Cyclic voltammetry (CV): The experiments were carried out in a custom-made three-electrode cell using a PGSTAT 302N (Metrohm Autolab) or a PGSTAT 128N (Metrohm Autolab). A glassy carbon disk (diameter: 1.6 mm) served as the working electrode and a platinum wire as the counter electrode. The glassy carbon disk was polished using polishing alumina suspension (0.05 μm) prior to each experiment. As reference, a $Ag/AgNO_3$ electrode (silver wire in 0.1 M NBu_4ClO_4/CH_3CN solution; $c(AgNO_3) = 0.01$ M; $E_0 = -87$ mV vs. ferrocene/ferrocenium couple)[22] was used, and this compartment was separated from the rest of the cell with a Vycor frit. NBu_4ClO_4 (0.1 M, electrochemical grade) was employed as supporting electrolyte in an acetonitrile-water mixture (8:1, vol./vol.). The electrolyte was purged with Ar for at least 5 min prior to recording. In order to account for the *iR* drop at high catalytic currents, positive feedback *iR* compensation was used. The resistance *R* was determined by electrochemical impedance spectroscopy prior to each experiment. Background corrections were made by subtracting the blank voltammograms from the CVs of the analytes.

Controlled potential electrolysis (CPE): The electrolyses were carried out in an H-type divided cell using a Vionic Potentiostat (Metrohm). A size exclusion membrane (regenerated cellulose, MW cut-off: 1 kDa, Merck) was used as a separator, a carbon roving wrapped around a PTFE sheet as a working electrode, and a Pt sheet as a counter electrode. A solution of 0.1 M NBu_4ClO_4 in CH_3CN/H_2O (8:1) served as the electrolyte, whereby 75 mM 4-methoxybenzyl alcohol, 110 mM 1-methylimidazol, and 5 mol-% TPMA (with respect to starting material and TEMPO units) were added to the anolyte. The anolyte and catholyte solutions (10 mL each) were prepared separately and filled simultaneously into the corresponding half-cells with syringes. During electrolysis, the working electrode potential was maintained at 0.55 V vs. Ag/0.01 M $AgNO_3$ using the same reference electrode as described for the cyclic voltammetry experiments. The yields were determined with a calibrated GC-FID (Trace 1310, Thermo Fisher) equipped with a HP-5 column (Agilent) using an internal standard (1,3,5-trimethoxy benzene).

Acknowledgements

This work has been funded by the German Research Foundation (DFG, project no. FR 3848/2-1). The author is grateful for funding by the DFG Heisenberg Program (FR 3848/4-1). Open Access funding enabled and organized by Projekt DEAL.

Conflict of Interest

The authors declare no conflict of interest.

Data Availability Statement

The data that support the findings of this study are available in the supplementary material of this article.

Keywords: electrosynthesis · electrocatalysis · mediators · redox-active polymers · TEMPO

[1] a) R. Francke, R. D. Little, *Chem. Soc. Rev.* **2014**, *43*, 2492–2521; b) L. F. T. Novaes, J. Liu, Y. Shen, L. Lu, J. M. Meinhardt, S. Lin, *Chem. Soc. Rev.* **2021**, *50*, 7941–8002.
[2] a) N. Kaeffer, W. Leitner, *JACS Au* **2022**, *2*, 1266–1289; b) L. Ackermann, *Acc. Chem. Res.* **2020**, *53*, 84–104; c) C. Ma, P. Fang, T.-S. Mei, *ACS Catal.* **2018**, *8*, 7179–7189; d) A. Jutand, *Chem. Rev.* **2008**, *108*, 2300–2347.
[3] a) J. Strehl, G. Hilt, *Org. Lett.* **2019**, *21*, 5259–5263; b) J. C. Siu, N. Fu, S. Lin, *Acc. Chem. Res.* **2020**, *53*, 547–560.
[4] a) P. Qian, Z. Zha, Z. Wang, *ChemElectroChem* **2020**, *7*, 2527–2544; b) N. Dagar, P. P. Sen, S. R. Roy, *ChemSusChem* **2021**, *14*, 1229–1257; c) F. Lian, K. Xu, C. Zeng, *Chem. Rec.* **2021**, *21*, 2290–2305.
[5] a) C. Y. Cai, X. M. Shu, H. C. Xu, *Nat. Commun.* **2019**, *10*, 4953; b) Y. S. Park, R. D. Little, *J. Org. Chem.* **2008**, *73*, 6807–6815; c) N. N. Lu, N. T. Zhang, C. C. Zeng, L. M. Hu, S. J. Yoo, R. D. Little, *J. Org. Chem.* **2015**, *80*, 781–789.
[6] a) R. Francke, *Curr. Opin. Electrochem.* **2019**, *15*, 83–88; b) R. Francke, *Curr. Opin. Electrochem.* **2021**, *28*; c) M. Elsherbini, T. Wirth, *Chem. Eur. J.* **2018**, *24*, 13399–13407.
[7] a) J. E. Nutting, M. Rafiee, S. S. Stahl, *Chem. Rev.* **2018**, *118*, 4834–4885; b) M. Rafiee, Z. M. Konz, M. D. Graaf, H. F. Koolman, S. S. Stahl, *ACS Catal.* **2018**, *8*, 6738–6744; c) H. B. Zhao, P. Xu, J. Song, H. C. Xu, *Angew. Chem. Int. Ed.* **2018**, *57*, 15153–15156; *Angew. Chem.* **2018**, *130*, 15373–15376; d) J. C. Siu, J. B. Parry, S. Lin, *J. Am. Chem. Soc.* **2019**, *141*, 2825–2831.
[8] a) Y. Yuan, A. Lei, *Nat. Commun.* **2020**, *11*, 802; b) R. Francke, *Chimia* **2020**, *74*, 49–56; c) J. Yoshida, K. Kataoka, R. Horcajada, A. Nagaki, *Chem. Rev.* **2008**, *108*, 2265–2299; d) R. Francke, *Curr. Opin. Electrochem.* **2022**, *36*, 101111.
[9] a) T. Broese, R. Francke, *Org. Lett.* **2016**, *18*, 5896–5899; b) O. Koleda, T. Broese, J. Noetzel, M. Roemelt, E. Suna, R. Francke, *J. Org. Chem.* **2017**, *82*, 11669–11681; c) A. F. Roesel, T. Broese, M. Májek, R. Francke, *ChemElectroChem* **2019**, *6*, 4229–4237.
[10] a) T. Tajima, T. Fuchigami, *J. Am. Chem. Soc.* **2005**, *127*, 2848–2849; b) T. Tajima, T. Fuchigami, *Angew. Chem. Int. Ed.* **2005**, *44*, 4760–4763; *Angew. Chem.* **2005**, *117*, 4838–4841; c) T. Tajima, H. Kurihara, T. Fuchigami, *J. Am. Chem. Soc.* **2007**, *129*, 6680–6681; d) S. J. Yoo, L. J. Li, C. C. Zeng, R. D. Little, *Angew. Chem. Int. Ed.* **2015**, *54*, 3744–3747; *Angew. Chem.* **2015**, *127*, 3815–3818; e) T. Sawamura, S. Kuribayashi, S. Inagi, T. Fuchigami, *Adv. Synth. Catal.* **2010**, *352*, 2757–2760; f) M. Kuroboshi, K. Goto, H. Tanaka, *Synthesis* **2009**, 903–908.
[11] Another option is the immobilization of molecular catalysts on electrode surfaces for heterogeneously electrocatalyzed transformations as exercised in refs. [11a–d]. a) D. P. Hickey, R. D. Milton, D. Chen, M. S. Sigman, S. D. Minteer, *ACS Catal.* **2015**, *5*, 5519–5524; b) F. C. Macazo, D. P. Hickey, S. Abdellaoui, M. S. Sigman, S. D. Minteer, *Chem. Commun.* **2017**, *53*, 10310–10313; c) A. Das, S. S. Stahl, *Angew. Chem. Int. Ed.* **2017**, *56*, 8892–8897; *Angew. Chem.* **2017**, *129*, 9018–9023.
[12] B. Schille, N. O. Giltzau, R. Francke, *Angew. Chem. Int. Ed.* **2018**, *57*, 422–426; *Angew. Chem.* **2018**, *130*, 429–433.
[13] N. Mohebbati, A. Prudlik, A. Scherkus, A. Gudkova, R. Francke, *ChemElectroChem* **2021**, *8*, 3837–3843.
[14] Applications of redox-active polymers in bioelectrochemistry have been recently reviewed: a) M. Kaneko, K. Ishihara, S. Nakanishi, *Small* **2020**, *16*, 2001849; b) M. Yuan, S. D. Minteer, *Curr. Opin. Electrochem.* **2019**, *15*, 1–6. For selected applications in bioelectrocatalysis, see: c) M. Kanekoa, M. Ishikawa, J. Song, S. Kato, K. Hashimoto, S. Nakanishi, *Electrochem. Commun.* **2017**, *75*, 17–20; d) K. Hasan, M. Grattieri, T. Wang, R. D. Milton, S. D. Minteer, *ACS Energy Lett.* **2017**, *2*, 1947–1951; e) Y. S. Lee, M. Yuan, R. Cai, K. Lim, S. D. Minteer, *ACS Catal.* **2020**, *10*, 6854–6861; f) G. Pankratova, D. Pankratov, R. D. Milton, S. D. Minteer, L. Gorton, *Adv. Energy Mater.* **2019**, *9*, 1900215. For selected applications in biosensors, see: g) S. M. Oja, B. Feldman, M. W. Eshoo, *Anal. Chem.* **2018**, *90*, 1536–1541; h) A. Ruff, P. Pinyou, M. Nolten, F. Conzuelo, W. Schuhmann, *ChemElectroChem* **2017**, *4*, 890–897.
[15] Applications of redox-active polymers in energy storage have been recently reviewed: a) K.-A. Hansen, J. P. Blinco, *Polym. Chem.* **2018**, *9*, 1479–1516; b) A. A. Vereshchagin, A. Y. Kalnin, A. I. Volkov, D. A. Lukyanov, O. V. Levin, *Energies* **2022**, *15*; c) J. Kim, J. H. Kim, K. Ariga, *Joule* **2017**, *1*, 739–768. For an outstanding example of TEMPO-modified polymers in redox flow batteries, see: d) T. Janoschka, N. Martin, U. Martin, C. Friebe, S. Morgenstern, H. Hiller, M. D. Hager, U. S. Schubert, *Nature* **2015**, *527*, 78–81.
[16] J. B. Flanagan, S. Margel, A. J. Bard, F. C. Anson, *J. Am. Chem. Soc.* **1978**, *100*, 4248–4253.
[17] G. Nagarjuna, J. Hui, K. J. Cheng, T. Lichtenstein, M. Shen, J. S. Moore, J. Rodríguez-López, *J. Am. Chem. Soc.* **2014**, *136*, 16309–16316.
[18] K. Zhang, Y. Hu, L. Wang, J. Fan, M. J. Monteiro, Z. Jia, *Polym. Chem.* **2017**, *8*, 1815–1823.
[19] Direct comparison between the M_n values of the TPMA samples used in this study and the one from Ref. [12] is not possible, since different SEC systems and standards were used for molecular weight analysis.
[20] T. Janoschka, A. Teichler, A. Krieg, M. D. Hager, U. S. Schubert, *J. Polym. Sci. Part A* **2012**, *50*, 1394–1407.
[21] a) D. B. Thomas, A. J. Convertine, R. D. Hester, A. B. Lowe, C. L. McCormick, *Macromolecules* **2004**, *37*, 1735–1741; b) C. P. Jesson, C. M. Pearce, H. Simon, A. Werner, V. J. Cunningham, J. R. Lovett, M. J. Smallridge, N. J. Warren, S. P. Armes, *Macromolecules* **2017**, *50*, 182–191.
[22] V. V. Pavlishchuk, A. W. Addison, *Inorg. Chim. Acta* **2000**, *298*, 97–102.
[23] R. F. Winter, *Organometallics* **2014**, *33*, 4517–4536.
[24] J. Wang, in *Analytical Electrochemistry*, Wiley-VCH, **2006**.
[25] A. J. F. Bard, in *Electrochemical Methods. Fundamentals and Applications*, Wiley, **2001**.
[26] a) B. M. Johnson, R. Francke, R. D. Little, L. A. Berben, *Chem. Sci.* **2017**, *8*, 6493–6498; b) M. A. Pellow, T. D. P. Stack, C. E. D. Chidsey, *Langmuir* **2013**, *29*, 5383–5387; c) M. V. Sheridan, K. Lam, W. E. Geiger, *Angew. Chem. Int. Ed.* **2013**, *52*, 12897–12900; *Angew. Chem.* **2013**, *125*, 13135–13138.
[27] a) M. D. Lechner, K. Gehrke, E. Nordmeier, *Makromolekulare Chemie*, Springer, **2020**; b) S. F. Sun, *Physical Chemistry of Macromolecules*, John Wiley & Sons, **2004**.
[28] a) J.-M. Savéant, *Chem. Rev.* **2008**, *108*, 2348–2378; b) C. Costentin, J.-M. Saveant, *J. Phys. Chem. C* **2015**, *119*, 12174–12182; c) C. Costentin, J.-M. Savéant, *Phys. Chem. Chem. Phys.* **2015**, *17*, 19350–19359.
[29] a) Preconditions for validity of Equation (3) are, among others, rate limitation by a single chemical step. In the present catalytic cycle (see Ref. [29b]), the reaction between the alcohol and the anodically formed oxoammonium species is generally assumed to be the rate-limiting step, while comproportionation between $TEMPO^+$ and TEMPOH is fast and thermodynamically favorable (see Refs. [29c] and [29d]). Consequently, Equation (3) has been used before for kinetic analysis of anodic alcohol oxidations mediated by TEMPO derivatives (see Refs. [29e] and [29f]); b) M. F. Semmelhack, C. R. Schmid, D. A. Cortés, *Tetrahedron Lett.* **1986**, *27*, 1119–1122; c) S. Kishioka, T. Ohsaka, K. Tokuda, *Chem. Lett.* **1998**, *27*, 343–344; d) A. Israeli, M. Patt, M. Oron, A. Samuni, R. Kohen, S. Goldstein, *Free Radical Biol. Med.* **2005**, *38*, 317–324; e) M. Rafiee, K. C. Miles, S. S. Stahl, *J. Am. Chem. Soc.* **2015**, *137*, 14751–14757; f) M. Rafiee, B. Karimi, S. Alizadeh, *ChemElectroChem* **2014**, *1*, 455–462.
[30] During optimization of the electrolysis conditions in our previous work, carbon roving was identified as the material with the best performance in view of product yield and long-term stability toward passivation.

Manuscript received: August 31, 2022
Accepted manuscript online: November 25, 2022
Version of record online: January 24, 2023